

# Photocurable Pillar Arrays Formed via Electrohydrodynamic Instabilities

Michael D. Dickey,<sup>†</sup> Elizabeth Collister,<sup>†</sup> Allen Raines,<sup>‡</sup> Pavlos Tsiartas,<sup>†</sup> Tom Holcombe,<sup>†</sup>  
S. V. Sreenivasan,<sup>‡</sup> Roger T. Bonnecaze,<sup>†</sup> and C. Grant Willson<sup>\*,†</sup>

Departments of Chemical Engineering and Mechanical Engineering, University of Texas at Austin,  
Austin, Texas 78712

Received November 23, 2005. Revised Manuscript Received January 31, 2006

Low viscosity, photocurable liquids are demonstrated as ideal materials for the formation of pillar arrays generated spontaneously by field-assisted assembly. Pillars form spontaneously via electrohydrodynamic instabilities that arise from the force imbalance at a film–air interface generated by an applied electric field. Conventional polymer films form pillars slowly as a result of their relatively large viscosities and are often process-limited by a requirement of heat to modulate rheological properties. In contrast, low viscosity liquids require no heat and form pillars orders of magnitude faster, as predicted by theory. The resulting structures are preserved by photopolymerization, eliminating the lengthy heating–cooling cycle necessary to process most polymers. The combination of nearly instantaneous formation and rapid photocuring at room temperature is ideal for patterning. Epoxy, vinyl ether, acrylate, and thiol-ene systems were evaluated for pillar formation. Relevant material properties were characterized (viscosity, dielectric constant, interfacial energy, kinetics) to explain the phenomenological behavior of each system during electrohydrodynamic patterning. The thiol-ene system formed pillar arrays nearly instantaneously and cured rapidly under ambient conditions. These are nearly ideal characteristics for pillar formation.

## Introduction

As photolithography approaches fundamental physical barriers, interest in alternative patterning techniques has grown. Directed-assembly patterning techniques are appealing because of their ability to harness natural phenomena to form useful structures. Recently, a directed-assembly technique has emerged that is capable of forming polymeric pillar arrays.<sup>1–5</sup> These arrays may find application in technologies such as micro-electro-mechanical systems, microfluidic devices, patterned magnetic media, and photonic band gap materials.<sup>6,7</sup>

The physical basis for the formation of the pillars is the amplification of film undulations by a destabilizing force, such as an electric field.<sup>1</sup> Experimentally, this is achieved by positioning an electrode above a thin film on a grounded substrate, a structure which resembles a parallel plate capacitor. Pillar formation occurs when the destabilizing

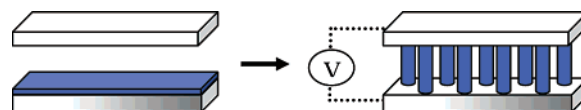


**Figure 1.** Depiction of the electrohydrodynamic instability phenomenon. An electric field destabilizes the film amplifying undulations until they span the capacitor gap.

electrostatic force overcomes the stabilizing effects of surface tension acting at the film–air interface. This force imbalance amplifies film fluctuations until they span the capacitor gap, as shown in Figure 1. Pillars only form when the temperature of the film is sufficiently high (i.e., above the polymer's glass transition temperature,  $T_g$ ) to permit flow of the polymer.

The dynamics of pillar formation have been modeled using three-dimensional nonlinear simulations<sup>8</sup> and linear stability analysis.<sup>1,3,6,8–12</sup> Linear stability analysis accounts for the forces acting on the film interface to determine the fastest mode of growth, providing a tool that can be used to predictably tune the characteristic spacing of the pillars. This analysis also predicts an exponential growth rate, with the time scale of pillar formation proportional to viscosity. These predictions have been verified experimentally in the early stages of undulation growth.<sup>13</sup> Thus, theory suggests that low-viscosity materials are ideal for rapid pillar array formation.

\* To whom correspondence should be addressed. E-mail: willson@che.utexas.edu.

<sup>†</sup> Department of Chemical Engineering.

<sup>‡</sup> Department of Mechanical Engineering.

- (1) Schaffer, E.; Thurn-Albrecht, T.; Russell, T. P.; Steiner, U. *Nature (London)* **2000**, 403 (6772), 874–877.
- (2) Chou, S. Y.; Zhuang, L. *J. Vac. Sci. Technol., B* **1999**, 17 (6), 3197–3202.
- (3) Schaffer, E.; Thurn-Albrecht, T.; Russell, T. P.; Steiner, U. *Europhys. Lett.* **2001**, 53 (4), 518–524.
- (4) Lin, Z.; Kerle, T.; Baker, S. M.; Hoagland, D. A.; Schaffer, E.; Steiner, U.; Russell, T. P. *J. Chem. Phys.* **2001**, 114 (5), 2377–2381.
- (5) Chou, S. Y.; Zhuang, L.; Deshpande, P.; Chen, L.; Sun, X. *Polym. Prepr. (Am. Chem. Soc., Div. Polym. Chem.)* **2000**, 41 (1), 78.
- (6) Pease, L. F.; Russel, W. B. *J. Chem. Phys.* **2003**, 118 (8), 3790–3803.
- (7) Yan, X.; Liu, G.; Dickey, M.; Willson, C. G. *Polymer* **2004**, 45 (25), 8469–8474.

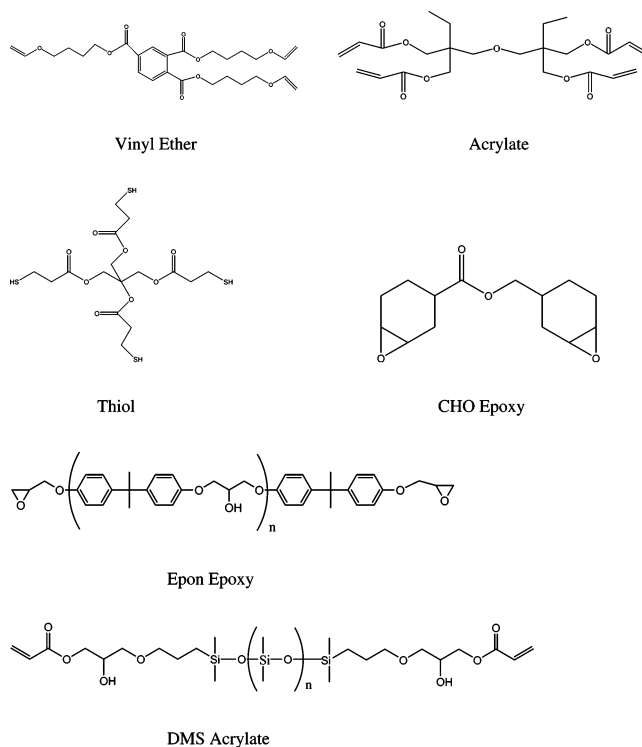
- (8) Verma, R.; Sharma, A.; Kargupta, K.; Bhaumik, J. *Langmuir* **2005**, 21 (8), 3710–3721.
- (9) Herminghaus, S. *Phys. Rev. Lett.* **1999**, 83 (12), 2359–2361.
- (10) Pease, L. F., III; Russel, W. B. *Langmuir* **2004**, 20 (3), 795–804.
- (11) Lin, Z.; Kerle, T.; Russell, T. P.; Schaffer, E.; Steiner, U. *Macromolecules* **2002**, 35 (10), 3971–3976.
- (12) Pease, L. F.; Russel, W. B. *J. Non-Newtonian Fluid Mech.* **2002**, 102 (2), 233–250.
- (13) Leach, K. A.; Lin, Z.; Russell, T. P. *Macromolecules* **2005**, 38 (11), 4868–4873.

**Table 1. Advantages of Low-Viscosity Photocurable Materials for Each Processing Step**

processing step	polymeric pillars	photocurable pillars
1. sample preparation	heat film above $T_g$	room temperature
2. apply e-field	high viscosity, slow pillar formation	low viscosity, rapid pillar formation
3. solidify structures	cool sample below $T_g$	rapid photo-polymerization
4. processing time	hours	seconds
5. final structures	residual material between pillars	no residual material between pillars

Electrohydrodynamic patterning requires a fluid material during pillar formation and a mechanism to lock the structures into place post-formation. In prior work, pillars have only been formed from polymer films, such as polystyrene, poly(methyl methacrylate), and polyisoprene.<sup>1–6,10–12</sup> With polymeric materials, pillar formation is accomplished using heat to modulate the rheological properties of the material. The polymer must be first heated above its  $T_g$  to allow it to flow and subsequently cooled to preserve the structures that are formed. The time scale of formation can be lengthy because of the high melt viscosities<sup>10,14</sup> and the accompanying heating–cooling cycle. Heating also limits the ability to predictably control the characteristic spacing due to distortion of geometry and thermal flux.<sup>15,16</sup> Linear stability analysis predicts that replacing polymeric films with liquids will reduce the time scale of pillar formation by several orders of magnitude, as a result of the substantial decrease in viscosity. Using photocurable liquids eliminates the heating–cooling cycle because the structures are fixed by photocuring. The photocuring process produces mechanically stable cross-linked polymeric columns. In many patterning applications, it is desirable to leave no residual material between patterned features. In contrast to polymeric pillars,<sup>1</sup> photocurable liquids generally leave very little residual material between the pillars (for example, see Figure 5). This is likely due to a combination of viscous and surface effects, both of which factor into surface wetting dynamics. The advantages of photocurable pillars are summarized in Table 1.

In this paper, we report the behavior of various photopolymerizable systems under electrohydrodynamic conditions. Initial material selection was based upon several processing requirements. The material must form a film that remains stable for the duration of the experiment but form pillars rapidly when exposed to the electric field. Thus, the material should be nonvolatile yet have a relatively low viscosity ( $\sim 1$  Pa·s). The material must photopolymerize rapidly, requiring highly reactive molecules with high mobility. Molecules with multifunctionality were favored to ensure mechanical stability of the columnar structures after curing. Preference was given to commercially available materials because of their accessibility. We auditioned a variety of photocurable reaction mechanisms and functional groups that were chosen to represent a range of physical

**Chart 1. Functional Materials Studied**

properties such as surface energy, viscosity, and dielectric constant. This study provides a basis for future rational material selection for photocurable electrohydrodynamic patterning.

## Experimental Section

**Materials.** The materials studied are illustrated in Chart 1. Acryloxy terminated poly(dimethylsiloxane) (DMS) was purchased from Gelest (Morrisville, PA). Tris[4-(vinyl-oxy)-butyl] trimellitate (vinyl ether), pentaerythritol tetrakis(3-mercaptopropionate) (thiol), di(trimethylolpropane)tetraacrylate (acrylate), and 3,4-epoxycyclohexylmethyl-3,4-epoxycyclohexanecarboxylate (CHO epoxy) were purchased from Aldrich (Milwaukee, WI). Bisphenol A diglycidyl ether (Epon epoxy, Epon 828) was purchased from Polysciences (Warrington, PA). The following materials were generously donated by their manufacturers: Darocur 4265 photoinitiator (CIBA, Basel, Switzerland) and Cyacure UVI-6992 photoinitiator (Dow/Union Carbide, Houston, TX). UVI-6992 is a mixture of (thiodi-4,1-phenylene)bis[diphenylsulfonium] bis[hexafluorophosphate] and diphenyl[4-(phenylthio)phenyl]-sulfonium hexafluorophosphate.

Solutions were formulated to produce an  $\sim 800$  nm film under reasonable spin casting conditions (2000–3500 rpm). Film thicknesses were measured by ellipsometry (Woollam WVASE32) and profilometry (Tencor Alpha-Step 200). A list of the material classes studied and the formulations for each class are shown in Table 2.

In addition to the material classes listed in Table 2, other photocurable materials were considered. Derivatives of cinnamic acid are known to undergo [2+2] photodimerization, an appealing reaction because of its reversibility and insensitivity to ambient oxygen. A difunctional cinnamate

(14) Leach, K. A.; Gupta, S.; Dickey, M. D.; Willson, C. G.; Russell, T. P. *Chaos* **2005**, *15* (4), 047506.

(15) Schaffer, E.; Harkema, S.; Roerdink, M.; Blossey, R.; Steiner, U. *Adv. Mater.* **2003**, *15* (6), 514–517.

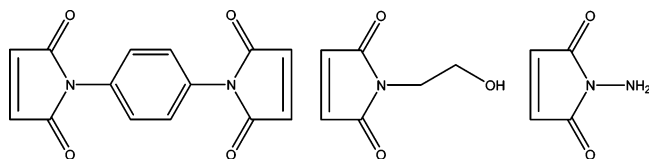
(16) Schaffer, E.; Harkema, S.; Blossey, R.; Steiner, U. *Europhys. Lett.* **2002**, *60* (2), 255–261.

Table 2. Materials Formulations

material class	component 1	component 2	initiator	reaction mechanism
thiol vinyl ether	17.5 wt % thiol	17.5 wt % vinyl ether	N/A	step radical
vinyl ether	30 wt % vinyl ether	N/A	5 wt % Cyracure	cationic
thiol	17.5 wt % thiol	17.5 wt % acrylate	N/A	step radical
acrylate (DMS)	25 wt % DMS <sup>a</sup>	N/A	5 wt % Darocur	radical
epoxy	17.5 wt % Epon	17.5 wt % CHO	5 wt % Cyracure	ring opening cationic

<sup>a</sup> The DMS was formulated in toluene, all others in propylene glycol methyl ether acetate casting solvent.

was synthesized by reacting 4,8-bis(hydroxymethyl)tricyclo-[5.2.1.0.2.6]decane with an excess of cinnamoyl chloride. The product is a viscous liquid. Unfortunately the time to sufficiently cross-link the material was found to be on the order of 1 h, consistent with other studies on polymers with pendant cinnamate groups.<sup>17,18</sup> This increase in processing time offset one of the biggest advantages of using photocurable materials, and thus cinnamates were removed from consideration. Maleimides, another common photocurable material, were also preliminarily investigated. Maleimides can act both as photoinitiators and as comonomers with various donor monomers including vinyl ethers. Various monofunctional and difunctional maleimides were synthesized but were found to be solids that were insoluble in the vinyl ether comonomers and thus inappropriate for this study. Representative maleimide structures are shown below.



Surface energies were measured using a Rame-Hart goniometer in pendant drop mode. The images from this instrument were analyzed using FTA2000, a software package donated by First Ten Ångströms. The dielectric constant was measured at room temperature using a Hewlett-Packard Impedance Analyzer (HP 4192A) with a Hewlett-Packard dielectric test fixture (HP 16451B) over three capacitor gaps. The viscosity was measured using a cone and plate rheometer (Physica MCR 300, 1° cone Anton Paar part no. 79040) at room temperature, calibrated with an oil of known viscosity.

The kinetics of polymerization were measured for each materials system using real-time Fourier transform infrared (RTIR) spectroscopy (Nicolet Magna-IR 550). RTIR utilizes in situ IR measurements to track the disappearance of functional groups during photocuring.<sup>19,20</sup> The IR was operated at a 4 cm<sup>-1</sup> resolution and four scans per spectrum with a collection time of 1.5 s per spectrum. Samples were prepared by spin-casting films on aluminum-backed, double-

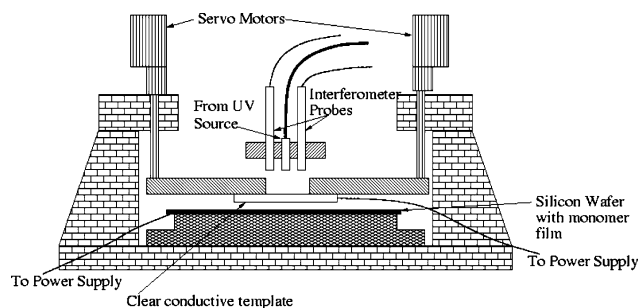


**Figure 2.** Active gap tool schematic. Three interferometer probes (note: only two are shown in the figure) are used to non-invasively measure the gap between the template and substrate. Servo motors actively position the template until planarity is achieved using feedback from the probes.

polished silicon wafers. The films were irradiated with a mercury lamp (EFOS Novacure) at 3.5 mW/cm<sup>2</sup>, an intentionally low intensity such that differences in the kinetics could easily be discerned. The relative functional group concentration was determined by measuring the peak height as a function of time.

**Experimental Procedure.** Pillars were formed using a custom-built machine designed for studying electrohydrodynamic instabilities, henceforth referred to as the active gap tool. A schematic of the active gap tool is shown in Figure 2. This tool, which will be described in greater detail in a separate manuscript, utilizes servo motors to position an optically flat fused silica template parallel to a silicon wafer that is held stationary by a grounded vacuum chuck. White light interferometry was used to measure and control the air gap between the wafer and the fused silica template. The interferometer also measures the film thickness, providing a valuable tool for measuring the approximate time scale of pillar formation, which is defined as the amount of time required for the pillars to span the gap. The fused silica template was coated with a thin layer of indium tin oxide (ITO) by electron-beam evaporation to provide a transparent, conducting surface. The templates were surface treated by silylation to aid release of the pillars from the upper electrode after curing. Load cells in the tool were used to measure the pillar–electrode release force.

Doped silicon wafers were used as substrates for the films, and the total substrate to upper electrode gap was set to ~3 μm. The gaps, measured by interferometry in real time, were verified by measuring the final pillar heights using scanning electron microscopy (SEM) analysis. Once the gap was set using the active gap tool, pillars were formed by applying 40 V across the electrodes. The pillars were photocured by exposure to a mercury lamp (EFOS Novacure).

In addition to the aforementioned tool, another technique was utilized to study pillar formation, an approach used by many other groups who study electrohydrodynamic instabilities.<sup>1–5</sup> This method relies on a physical spacer to create the capacitor gap. Spacers were created by etching a recess into a glass slide and depositing a thin layer of metal to create the electrode. The disadvantage of this method is that the spacer contacts the film, disrupting an otherwise smooth surface. This method was useful for monitoring and recording the formation of pillars in situ and in real time using optical microscopy, an option currently unavailable on the active gap tool as a result of geometry restrictions.

(17) Lendlein, A.; Jiang, H.; Juenger, O.; Langer, R. *Nature* **2005**, 434 (7035), 879–882.

(18) Ali, A. H.; Srinivasan, K. S. V. *Polym. Int.* **1997**, 43 (4), 310–316.

(19) Dickey, M. D.; Burns, R. L.; Kim, E. K.; Johnson, S. C.; Stacey, N. A.; Willson, C. G. *AIChE J.* **2005**, 51 (9), 2547–2555.

(20) Decker, C. *Macromol. Rapid Commun.* **2002**, 23 (18), 1067–1093.



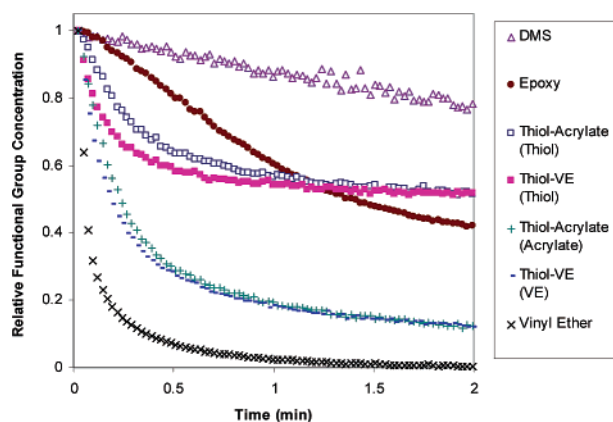


**Figure 3.** RTIR kinetic profile for each material system, representing the consumption of each respective functional group with time due to polymerization ( $3.5 \text{ mW/cm}^2$ ). In the multicomponent systems, the specific functionality is listed in brackets. Note that VE is short for vinyl ether.

**Table 3. Material Properties**

material	viscosity (Pa·s)	surface energy (dyn/cm)	dielectric constant
thiol vinyl ether	0.471	40.0	8.55
vinyl ether	0.286	39.5	7.92
thiol acrylate	0.593	34.8	9.89
DMS acrylate	0.101	20.8	3.91
epoxy	1.786	45.2	10.41

## Results and Discussion

The properties of the primary materials studied are summarized in Table 3. The viscosities span an order of magnitude, and the surface energy varies by a factor of 2 across the material set, as does the dielectric constant. Most of the materials have a relatively high dielectric constant, a trait that is favorable for pillar formation because it increases the destabilizing electrostatic force. The relatively low viscosity of the materials is also favorable for pillar formation because the time scale of formation is directly proportional to viscosity. Similarly, low surface energy is favorable for rapid pillar formation due to the decreased stabilizing interfacial forces. On the basis of these scaling arguments rooted in linear stability analysis,<sup>13</sup> the DMS should form the fastest and the epoxy should take the longest to form.

Polymerization kinetics for each material are shown in Figure 3. As expected, the DMS has extremely slow cure kinetics because the radical mechanism by which it cures is strongly inhibited by oxygen.<sup>19,21</sup> Pillars have a high surface area-to-volume ratio, making them particularly susceptible to inhibition by oxygen diffusion during irradiation well after the initial dissolved oxygen is consumed. The epoxy system also cured slowly. Although epoxies are generally very reactive, the high viscosity of the epoxy formulation limits the reaction rate. In highly viscous systems, it is difficult for reactive centers to find unreacted functional groups to propagate the polymerization.

The vinyl ether polymerizes via a cationic mechanism and has the fastest polymerization kinetics of all the materials studied. The low viscosity of the material combined with the relatively large functional group concentration results in a rapid polymerization. The thiol vinyl ether and thiol

acrylate polymerizations are also very fast, as seen in Figure 3. That reaction proceeds via a free-radical step growth mechanism, in which a thiyl radical first inserts into the ene, followed by hydrogen abstraction from another thiol to generate a new thiyl radical.<sup>22</sup> The presence of the thiol acts like a chain transfer agent and reduces the deleterious effects of oxygen seen in traditional radical systems. The thiol does not proceed to the same extent of conversion as the acrylate or vinyl, implying that some ene homopolymerization takes place. Although virtually any ene will participate in the free radical reaction with thiol, vinyl ethers and acrylates were chosen because of their commercial availability, viscosity, and relatively high reactivity. These systems are particularly interesting because they do not require an initiator, resulting in a simplified formulation.<sup>23–25</sup>

As expected, all of the materials studied formed pillars rapidly under the influence of the electric field. The thiol vinyl ether exhibited the best characteristics for pillar formation. A top-down optical micrograph of typical thiol vinyl ether pillars is shown in Figure 4. The average pillar diameter is  $17.8 \mu\text{m}$  as determined using Scion image analysis software. The characteristic spacing was found to be  $\sim 30 \mu\text{m}$  using two-dimensional fast Fourier Transform.<sup>11</sup> Linear stability analysis predicts the characteristic spacing of the fastest growing mode to be  $\sim 40 \mu\text{m}$  for these conditions (gap  $2.5 \mu\text{m}$ ). The difference between experimental and theoretical values is within experimental error, but the smaller experimental value could be indicative of a leaky dielectric.<sup>10,12</sup> A more in-depth analysis of the characteristic spacing is underway, in which the critical parameters are being systematically varied to determine if the characteristic spacing of low viscosity materials follows linear stability predictions.

On the basis of in situ growth observations, pillars formed either instantaneously or within seconds, with the exception being the epoxy which took 30–60 s to form. The center-to-center spacing of the resulting structures ( $\sim 30 \mu\text{m}$ ) closely matched the spacing of the initial undulations induced by the electric field. However, pillar growth was somewhat stochastic as fluctuations did not grow into columns simultaneously, consistent with observations by Leach et al.<sup>13</sup> In addition to the observed spinodal instabilities, there was also evidence of nucleated growth. This observation is consistent with experiments and modeling done by other groups on polymeric systems.<sup>1–5,8</sup> In nucleated growth, a pillar initially forms at a nucleation site, followed by growth of concentric rings of pillars. In a similar type of phenomenon, growth fronts were observed in regions initiated near edges. Sharp spatial gradients in the electrostatic force at the electrode edge cause this nucleation, as predicted by modeling.<sup>8</sup> These fronts typically propagate toward the center of the sample until they impinge upon another growth region. As a result,

(22) Jacobine, A. F. In *Radiation Curing in Polymer Science and Technology III, Polymerization Mechanisms*; Fouassier, J. P., Rabek, J. F., Eds.; Elsevier Applied Science: London, 1993.

(23) Cramer, N. B.; Davies, T.; O'Brien, A. K.; Bowman, C. N. *Macromolecules* **2003**, *36* (12), 4631–4636.

(24) Cramer, N. B.; Scott, J. P.; Bowman, C. N. *Macromolecules* **2002**, *35* (14), 5361–5365.

(25) Cramer, N. B.; Reddy, S. K.; Cole, M.; Hoyle, C.; Bowman, C. N. *J. Polym. Sci., Part A: Polym. Chem.* **2004**, *42* (22), 5817–5826.

(21) Decker, C.; Jenkins, A. D. *Macromolecules* **1985**, *18* (6), 1241–1244.

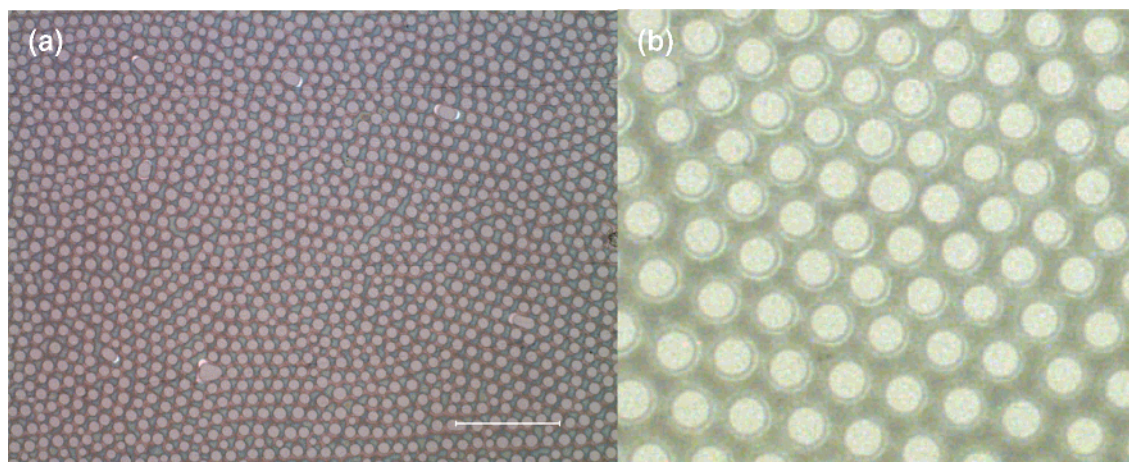


**Figure 4.** Optical micrograph of thiol vinyl ether pillars. (a) Overview of the pillar array that shows local order but lacks long range order (scale bar 200  $\mu\text{m}$ ). (b) Enlarged view of local order near the electrode edge (width of image  $\sim 250 \mu\text{m}$ ).

there were regions with local hexagonal close-packed order but no long range order. The lack of long range order in photocurable systems is consistent with published images of polymeric pillars.<sup>1–5,11,13,26,27</sup> In agreement with theory,<sup>8</sup> local ordering was best toward the electrode edges, as shown in Figure 4b. It appears that packing occurs due to the rings of depleted material surrounding each pillar and by the nature of the spinodal instability.

Although low viscosity films form uniform pillars rapidly, the resulting structures are only in a local energy minima. The overall energy of the system can be lowered by pillars merging. A few merged pillars (less than 1%) can be seen in Figure 4. This tendency was minimized by the use of thiol vinyl ether and was the worst with DMS because of its low viscosity and surface energy. Obviously, the merging of pillars can be minimized by reducing the lag time between pillar formation and photocuring. Modeling has shown that pillar coalescence is largely a function of the air gap to film thickness ratio, where values greater than 3 form quasi-stable columns.<sup>8</sup> This ratio was  $\sim 4$  in all of the experiments performed in this study; thus, coalescence was not favored. Despite this favorable configuration, a number of factors could lead to pillar agglomeration: heterogeneities on the electrode surface, liquid bridges between structures resulting from residual material, pillar to pillar contact due to upper electrode wetting, and distortions of the electric field resulting from structure formation. In the case of a wedged capacitor geometry, the pillars could move to minimize interfacial energy. This was ruled out as a possibility based on real-time monitoring of pillar formation because the pillars did not move in concert in any one direction.

The presence of residual material between pillar structures can be seen via optical microscopy and via cross-sectional SEM. All of the materials studied left little to no residual material. Figure 5 shows the cleaved edge of a silicon substrate, and the edges of a pillar can be seen clearly. No residual layer exists surrounding the base of the pillar, a trait that is highly favorable for transferring patterns to the

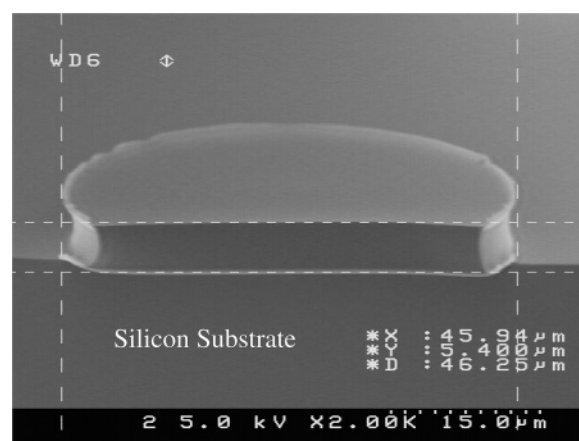


**Figure 5.** Tilt-angle SEM image of a cleaved pillar on top of a cleaved silicon substrate, demonstrating the extremely small residual layer surrounding the pillar.

underlying substrate. The epoxy was the only material that left a significant residual layer between structures. The exact reasons for this are unclear, although the larger resistance to flow at the silicon–film interface due to the higher viscosity of the epoxy is likely a factor. Favorable interactions between the epoxy and the substrate may also lead to the observed residual material.

In the following section, the advantages and disadvantages of each materials class will be discussed, with a particular focus on the effects of material properties on pillar formation.

**Epoxy.** The epoxy had the most processing limitations of all the materials studied. The high viscosity caused the pillars to form slowly (30–60 s). As seen in Figure 3, the epoxy system cures slower than the vinyl ether system despite the use of the same initiator. The slower epoxy polymerization kinetics could be due to the larger viscosity of the reaction medium, the lower functional group reactivity, and possibly poor initiator compatibility. Crivello et al. have shown that onium metal halides are effective initiators for epoxy polymerizations.<sup>28,29</sup> These initiators were not investigated because optimizing the reaction kinetics was not a priority of this study. The epoxy only cures using sub-300 nm UV

(26) Chou, S. Y.; Zhuang, L.; Guo, L. *Appl. Phys. Lett.* **1999**, 75 (7), 1004–1006.

(27) Lin, Z.; Kerle, T.; Russell, T. P.; Schaeffer, E.; Steiner, U. *Macromolecules* **2002**, 35 (16), 6255–6262.

(28) Falk, B.; Zonca, M. R., Jr.; Crivello, J. V. *J. Polym. Sci., Part A: Polym. Chem.* **2005**, 43 (12), 2504–2519.

(29) Bulut, U.; Crivello, J. V. *Macromolecules* **2005**, 38 (9), 3584–3595.



light because of the absorbance characteristics of the photoacid generator (PAG), adding additional processing requirements to the exposure source and UV transparent template. The fused silica templates used in this study were sufficiently transparent to transmit sub-300 nm light; however, the absorbance of the PAG can be tuned to other wavelengths,<sup>30</sup> or the PAG can be sensitized by adding appropriate chromophores if necessary.<sup>31</sup> As previously discussed, the epoxy pillars had a significant amount of residual material between structures. The epoxies also displayed the largest separation force required to release the pillars from the upper electrode ( $\sim 30$  lb versus  $\sim 12$  lb for the other materials). This was not surprising because epoxies are often used as adhesives.

**Vinyl Ethers.** Vinyl ethers are appealing because they photocure rapidly and the cationic polymerization mechanism is insensitive to oxygen.<sup>32</sup> However, they can be inhibited by ambient species such as moisture and base. Unfortunately, most commercially available vinyl ethers are volatile and, therefore, do not form stable films.<sup>20</sup> The few vinyl ethers that are capable of forming stable films tend to have limited ability to dissolve PAGs necessary for initiating the cationic mechanism. The use of a PAG adds the processing requirement of either sub-300 nm irradiation or photosensitization to initiate the polymerization. Over 10 different PAGs, including common PAGs such as triphenylsulfonium SbF<sub>6</sub> and bis-*p-tert*-butylphenyliodonium triflate, were screened for compatibility, and none were readily soluble in the vinyl ether. The Cyacure initiator used in this system is a liquid, formed by dissolving a PAG into a solvent. Therefore, the possibility of the PAG coming out of solution during spin casting exists but did not appear to be a problem because the spin cast films were smooth. However, there was evidence of solution instability over a period of a few days. We are aware of custom PAGs that are compatible with vinyl ethers.<sup>30</sup>

The vinyl ether films formed pillars very rapidly ( $\sim 5$  s). During separation, the pillars underwent cohesive failure rather than adhesive failure, resulting in rough and distorted features. Residue remained on the template (both ITO and Cr electrodes) despite surface treatment. This residue could not be removed by UV–ozone treatment or oxygen plasma, ultimately destroying the templates. The residue on the template affected subsequent experiments, causing pillars to migrate as a result of heterogeneities of the surface energy. X-ray photoelectron spectroscopy analysis of the contaminated surface revealed the presence of atomic species from the PAG.

**Acrylates.** As expected, the acrylates formed pillars very rapidly ( $< 1$  s) because of the low viscosity of the DMS material. The acrylate pillars also had the largest variation of pillar diameter, largely as a result of their tendency to migrate and merge after forming. The combination of low viscosity and low surface energy allowed the DMS to have

high mobility prior to curing. The result is an array of pillars with many different diameters (i.e., polydisperse). In situ growth observation confirmed that the DMS pillars form with a uniform diameter but rapidly merge to form larger pillar agglomerates.

The biggest disadvantage of using an acrylate system is that the radical polymerization mechanism is oxygen sensitive.<sup>19,21</sup> Curing the structures requires either an inert atmosphere or an intense irradiation dose. These multiple processing constraints make acrylates unappealing for processing.

**Thiol-ene.** Thiol-ene systems are desirable because they are insensitive to oxygen. The addition of a thiol to an ene (acrylate, vinyl ether, etc.) reduces the sensitivity to oxygen by acting as a chain transfer agent. Thus, the reaction mechanism for thiol-ene systems involves a step reaction using free radicals generated by irradiation, although the system does not require initiator.<sup>23–25</sup> Thiol-ene systems have been studied for many years,<sup>33–35</sup> but there has been a recent surge of interest in these materials because of their many desirable properties.<sup>36</sup> Both the thiol acrylate and thiol vinyl ether materials performed well during pillar formation. They formed pillars rapidly ( $< 5$  s) and cured rapidly. One disadvantage of the thiol acrylate system is that thin films require sub-300 nm irradiation to cure. Bulk thiol acrylate cures rapidly with light above 300 nm; however, thin films only cure when protected from the ambient air by a coverslip. The implication is that when  $> 300$  nm light is used for photocuring, radicals are generated at an insufficient rate to keep up with inhibition by diffusing oxygen. Cramer et al. demonstrated that thiol-ene photopolymerizations proceed more readily at sub-300 nm wavelengths and undergo a wavelength-dependent initiation process.<sup>24,25</sup> This wavelength restriction can be avoided by adding a radical initiator (e.g., Darocur 4265), which detracts from the elegance of the initiator-less system. It should be noted that adding initiator ( $\sim 5$  wt %) to either of the thiol-ene systems dramatically increases the rate of polymerization ( $\sim 6$  s to reach 80% conversion versus  $\sim 45$  s in the initiator-less system).

Figure 6 is a SEM image of the thiol vinyl ether pillars, in which the pillars measure approximately  $2.5\ \mu\text{m}$  tall with a diameter of  $17\ \mu\text{m}$ . Again, a residual layer is undetectable, implying that all the material gets drawn into the columns. In general, the thiol vinyl ether displayed the most ideal properties for pillar formation of all the materials studied. The thiol vinyl ether cured at both sub-300 nm and  $> 300$  nm light, implying it is less sensitive to oxygen, which is consistent with vinyl ethers being one of the most reactive ene species in thiol-ene systems.<sup>36</sup> In addition to rapid pillar formation and curing, the thiol vinyl ether system showed almost no pillar merging tendencies under any conditions. This is rather remarkable considering the material properties of the thiol vinyl ether do not differ greatly from the other materials studied. We suspect that electrochemistry might

(30) Crivello, J. V.; Ahn, J. *J. Polym. Sci., Part A: Polym. Chem.* **2003**, *41* (16), 2570–2587.

(31) Wallraff, G. M.; Allen, R. D.; Hinsberg, W. D.; Willson, C. G.; Simpson, L. L.; Webber, S. E.; Sturtevant, J. L. *J. Imaging Sci. Technol.* **1992**, *36* (5), 468–476.

(32) Decker, C. *Polym. Int.* **1998**, *45* (2), 133–141.

(33) Morgan, C. R.; Magnotta, F.; Ketley, A. D. *J. Polym. Sci., Polym. Chem. Ed.* **1977**, *15* (3), 627–645.

(34) Morgan, C. R.; Ketley, A. D. *J. Polym. Sci., Polym. Lett. Ed.* **1978**, *16* (2), 75–79.

(35) Morgan, C. R.; Ketley, A. D. *J. Radiat. Curing* **1980**, *7* (2), 10–13.

(36) Hoyle, C. E.; Lee, T. Y.; Roper, T. J. *J. Polym. Sci., Part A: Polym. Chem.* **2004**, *42* (21), 5301–5338.

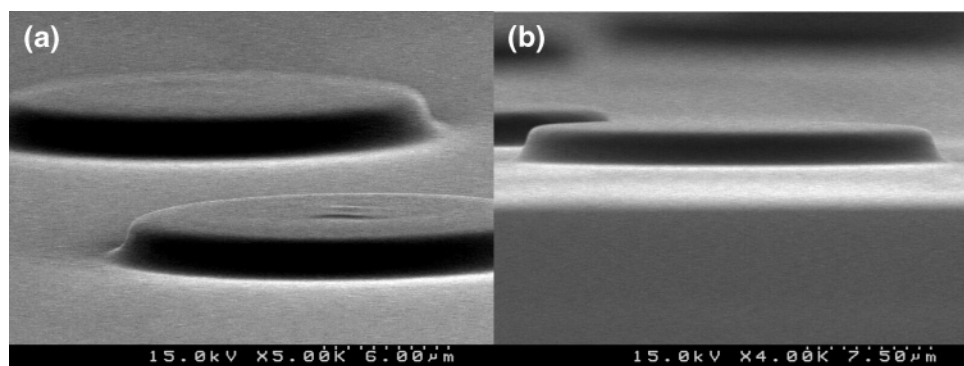


**Figure 6.** Tilt-view SEM image of thiol vinyl ether pillars.

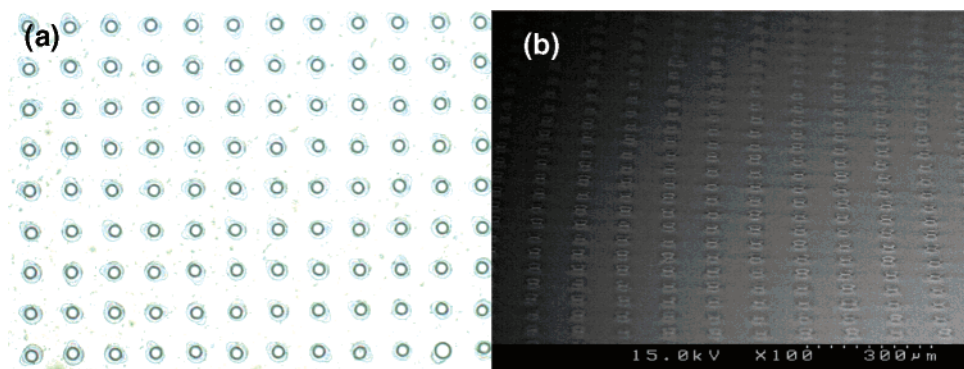


**Figure 7.** Thiol vinyl ether pillar arrays formed using a patterned electrode. (a) Optical micrograph of pillar arrays (image width 1.1 mm). (b) Tilt-view SEM image of the pillar array.

be playing a roll in the curing process, ultimately reducing the mobility of the thiol vinyl ether by inducing some level of polymerization as soon as the material spans the electrodes. A small current ( $\sim 25 \mu\text{A}/\text{cm}^2$ ) was detected during pillar formation, but this was not unique to the thiol vinyl ethers. However, the thiol vinyl ether pillars did cure in the absence of light when a 40 V potential was applied for 5 min. None of the other materials displayed this property. The mechanism is unclear, but preliminary cyclic voltametry studies show that the thiol rapidly forms disulfide bonds at low voltages ( $<1$  V), which points to a potential source of electrically generated radicals. This inadvertent yet fortuitous property of the thiol vinyl ether allows the pillars to be cured in the absence of light and minimizes the post-formation coalescence.

The only observed drawback of the thiol-ene system is that the solutions are unstable. They oligomerize in the absence of light on the time scale of days. To keep consistent performance, fresh solutions must be made frequently or an inhibitor must be added to the casting solutions.

As discussed previously, pillar arrays lack long range order. Patterned electrodes have been demonstrated as a technique to improve the long range order of pillars in polymeric systems.<sup>1,2</sup> Figure 7 provides evidence that this technique is effective for low-viscosity systems as well. An upper electrode with protruding  $50 \mu\text{m}$  posts on  $100 \mu\text{m}$  spacing was used to direct the formation of pillars. Pillars preferentially form at the protruding features because of the

locally higher electric field. Work is in progress examining the patterning length scale limits using this technique.

### Conclusions

The ability to form arrays of pillars using photocurable materials was demonstrated. The pillars form at room temperature, and the time scale of formation is orders of magnitude faster than high  $T_g$  polymers (seconds vs hours). A number of photopolymerizable materials with a variety of material properties were investigated. The thiol vinyl ether displayed many desirable properties for pillar formation. It forms pillars nearly instantaneously with minimal coalescence, cures rapidly without an initiator, and is insensitive to ambient species. Future work will focus on determining the dependence of the characteristic spacing as a function of system parameters.

**Acknowledgment.** We are grateful to Amanda Leach, Suresh Gupta, and Dr. Tom Russell for valuable assistance on the pillar formation process. We thank the Center for Nanomaterials at the University of Texas for use of the thermal evaporator. We thank the NSF for fellowship funding. Nelson Hu generously assisted with the dielectric constant measurements. Undergraduate research assistants Keris Allrich, Jarrett Woock, and Sumarlin Goh all contributed to this work. Thank you to the Texas Advanced Materials Research Center for funding.

CM052592W